NMR spectra since two distinct peaks (δ ~3.38, 3.78 ppm) caused by these protons are observed in CDCA vs. only one peak (δ ~3.45 ppm) caused by the same protons in UDCA. The fingerprint region of the spectrum (δ ~1–2.5 ppm) and the relative position of the C_{19} methyl peak with respect to that of the doublet caused by the C_{21} methyl group provide additional confirmation of the identity of the particular epimer. Accurate quantitative results are obtained from careful integration of the C_3 and C_7 methine proton peaks. The specific method of identification and quantitation described in this report provides an efficient alternative to the rather nonspecific identification and assay procedures by conventional techniques, some of which involve making derivatives of the bile acid epimers. This paper, which is the first publication of its kind dealing with the quantitation of steroids by NMR spectrometry, demonstrates that NMR spectrometry can be an excellent tool for assaying steroids.

ACKNOWLEDGMENT

The authors thank S. Moros for his comments and support, A. Mlodozeniec and J. Sheridan for their support, and L. Rubia for helpful discussion, and Mrs. J. Comment for typing the manuscript.

LITERATURE CITED

(1) J. N. Shoolery and M. T. Rogers, *J. Am. Chem. Soc.* **80**, 5121 (1958).
(2) N. S. Bhacca and D. H. Williams, "Applications of NMR Spectroscopy in Organic Chemistry, Illustrations from the Steroid Field", Holden-Day, San Francisco, Calif., 1964.

RECEIVED for review February 21, 1978. Accepted June 19, 1978.

Isotope-Ratio-Monitoring Gas Chromatography–Mass Spectrometry

D. E. Matthews[1] and J. M. Hayes*

Departments of Chemistry and Geology, Indiana University, Bloomington, Indiana 47401

A 750 °C cupric-oxide-packed combustion furnace is inserted between the gas chromatographic column outlet and a GC/MS interface attached to a computer-controlled beam-switching isotope ratio mass spectrometer. Monitoring of N_2 and CO_2 ion currents due to the combustion products allows continuous measurement of $^{15}N/^{14}N$ or $^{13}C/^{12}C$ ratios, providing directly comparable isotopic analyses for all eluting compounds regardless of composition and mass spectrometric behavior of the parent compounds. Carbon and nitrogen isotope ratios can be measured with a precision of 0.5% or better with 20 nmol of CO_2 or 100 nmol of N_2. Enrichments of ^{13}C and ^{15}N as low as 0.004 at. % excess can be detected.

Isotope ratios of carbon and nitrogen can be determined with very good precision (better than 0.1% relative standard deviation) by differential isotopic analysis of combustion products using the dual inlet, dual collector mass spectrometric technique developed by C. R. McKinney et al. (*1*), and with poor to good precision (10.0–0.5%, depending upon the conditions) by selected ion monitoring gas chromatography–mass spectrometry (SIM-GCMS) (2). The techniques are somewhat complementary, the former providing high precision but requiring relatively large samples, the latter handling smaller samples at the cost of reduced precision.

Differences between the approaches are fundamental, however, because the GCMS technique directly incorporates a process of sample purification and is capable of resolving mixtures of compounds, while conventional dual inlet, dual collector techniques require that even sample combustion, let alone any steps aimed at the resolution of mixtures, be performed off-line. In practical terms, the integral separation process gives the GCMS technique enormous advantages in the rate of sample throughput and in the confidence which can be placed in results which are intended to relate to individual, pure compounds. A second fundamental contrast involves the nature of the ion currents measured: the GCMS technique deals with large, multielement fragment ions, while the dual inlet, dual collector technique accepts only molecular ions of small species containing at most two elements. The advantage here lies decisively with the latter technique. Consider, for example, the problem of measuring nitrogen isotopic abundances in organic compounds by SIM-GCMS: an ionic species useable for nitrogen isotopic measurements must be identified in the spectrum of each compound of interest, and the resulting data must be corrected for (i) contributions due to other heavy isotopes (^2H, ^{13}C, ^{17}O), and (ii) possible contributions to the apparent ^{15}N abundances by other ionic species (e.g., fragment + H). The uncertainties associated with these corrections can seriously degrade the nitrogen isotopic measurements. On the one hand, natural isotopic abundance variations in ^{13}C, for example, could introduce significant errors. On the other hand, exclusion of errors due to the second correction could require the selection and careful study of as many as 20 different pairs of masses in a chromatogram involving 20 different compounds of interest.

Here we report on the capabilities of a new technique (*3*) aimed at combining the mixture-handling capacity and speed of SIM-GCMS with the isotopic clarity of the dual inlet, dual collector technique. The technique, which we term "isotope-ratio-monitoring gas chromatography–mass spectrometry" (IRM-GCMS), can measure nitrogen and carbon isotope ratios down to natural abundance levels for any organic component (or components) that can be resolved gas chromatographically. The IRM-GCMS system shown in Figure 1 is very similar to that described by Sano et al. (*3*): a gas chromatograph, a combustion oven, and a mass spectrometer, connected in series. The effluent from the gas chromatograph is quantitatively combusted to CO_2, N_2, H_2O, etc; a selective trap removes combustion products other than those of interest; and the effluent enters the mass spectrometer. Carbon isotope ratios are determined by mea-

[1] Present address, Department of Medicine, Washington University School of Medicine, St. Louis, Mo. 63110.

0003-2700/78/0350-1465$01.00/0

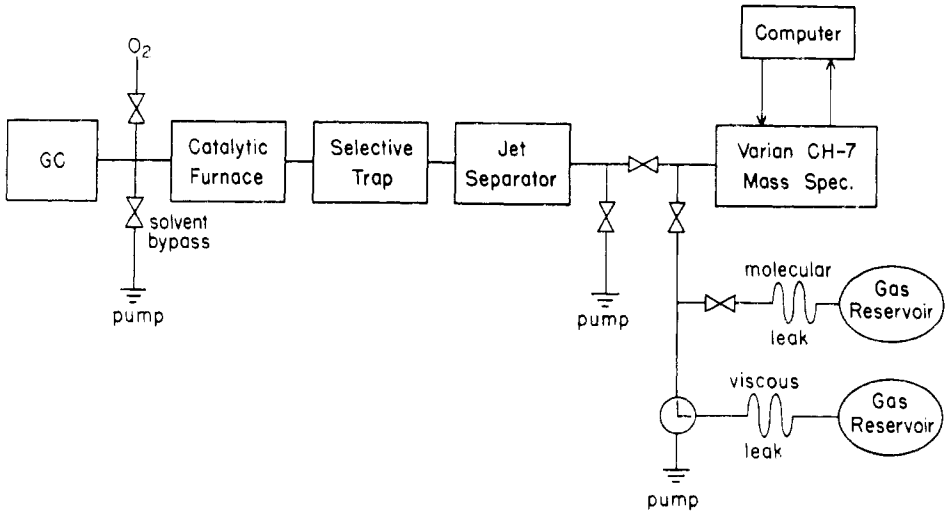

Figure 1. Block diagram of IRM-GCMS system

surement of the ion currents at masses 45 ($^{13}CO_2 + {}^{12}C^{16}O^{17}O$) and 44 ($^{12}CO_2$), while nitrogen isotopes are determined by measurements of the ion currents at masses 29 ($^{15}N^{14}N$) and 28 ($^{14}N_2$).

The combination of a gas chromatograph with a combustion oven is not new. In 1960, in order to normalize the detector response with regard to carbon number, the effluent from a gas chromatograph was passed through a combustion oven before entering a thermal conductivity detector (*4*). In the same year, the effluent from a gas chromatograph was combusted in order to allow on-line elemental analysis of GC peaks — the carbon/hydrogen ratio being determined from the CO_2/H_2 ratio after the water combustion product was reduced to hydrogen (*5*). In another use, a gas chromatograph–combustion oven combination followed by a proportional or ionization detector was reported for the measurement of carbon-14 (*6, 7*) and tritium abundances (*8*). The pioneering demonstration of the technique of IRM-GCMS (*3*) involved the determination of carbon-13 labeled drug metabolites.

EXPERIMENTAL

Apparatus. The mass spectrometer–computer system is a Varian CH-7 single focusing mass spectrometer interfaced to a Varian 620i minicomputer (*9*). The mass spectrometer accelerating voltage power supply can be scanned by the computer with 12-bit resolution from 3000 to 2700 V. The CH-7 is normally operated with an ionizing electron energy of 70 eV and an emission current of 100 μA. The CH-7 is tuned and the variable collector slit is adjusted to achieve broad flat-topped ion peaks with a resolution of 270 (10% valley definition). The electron multiplier is an ITT-F4074 16-dynode multiplier (ITT, Fort Wayne, Ind.) and is normally operated at a gain of 6×10^5. The electron multiplier signal-conditioning system, constructed at Indiana University according to the circuit of Woodruff and Malmstadt (*10*), employs a current amplifier followed by a current-to-frequency (I/F) converter. The gain of one stage of current-amplification is switch-selectable at X1, X10, or X100. The gain of another stage is either switch-selectable *or* computer-controllable at X1 or X100. The three-decade range is used to select the proper sensitivity; the two-decade range is used in the measurement of near-natural-abundance isotope ratios by selecting the X1 gain for the major isotope and the X100 for the minor. When the electron multiplier is set to the normal 6×10^5 gain, and the least sensitive gains are employed (X1 and X1), the I/F system produces one pulse for every 500 ions.

The Varian 620i computer employs 16-bit words, is equipped with 8192 words of magnetic core memory, and is programmed in assembly language. The system contains a drum, two magnetic tape drives, a Teletype, and a Tektronix 4010 CRT with hard copy unit. The computer controls the mass spectrometer accelerating voltage, inlet system valves, I/F amplifier (X1–X100 gain selection), and receives the I/F amplifier output pulse train via a 16-bit 300-MHz counter/clock/gate circuit (Varian MAT, Bremen, West Germany).

The gas chromatograph is a Hewlett-Packard 5700A gas chromatograph, fitted with a locally constructed glass-lined stainless steel injector designed for $^1/_8$-inch stainless steel GC columns. The injector is housed in an aluminum heating block and is supplied with a water-cooled septum holder. Helium (UHP) is used as the carrier gas.

A schematic diagram of the combustion system is shown in Figure 2. The combustion oven is connected to the water and carbon dioxide traps, and the traps are connected to the GCMS separator (Figure 2). The GCMS separator is a single-stage glass jet separator (Vacumetrics, Inc., Ventura, Calif.). The effluent from the jet separator can either be allowed to enter the CH-7 or can be diverted to a 1-inch baffled oil diffusion pump. In addition to the GCMS inlet, the CH-7 has an inlet for admitting gases from inlet systems incorporating molecular or viscous leaks. All valves in the system (as shown in Figure 1) are controlled by the computer.

Software. The IRM-GCMS computer program requires that the appropriate mass range ($27 < m/e < 30$ for N_2, $43 < m/e < 47$ for CO_2) be manually preset by adjustment of the magnetic field. The computer controls the system, first opening the proper leak to admit a sample of CO_2 or N_2 (depending on which isotopes are to be measured), then accurately determining the accelerating voltages corresponding to the centroids of the major and minor isotopic ion beams. When the operator signals that a GC injection has been made, the computer confirms that the GCMS inlet valve is closed, that the GCMS bypass valve is open, and that the solvent bypass valve (before the combustion oven) is open. After a delay for elution of the solvent peak, the solvent bypass valve is closed. Following a delay of approximately 1 min in order to allow stabilization of the flow through the combustion system, the GCMS bypass valve is closed and the GCMS inlet valve to the CH-7 is opened.

Before data acquisition begins, the centroid location of the major isotopic ion beam is automatically redetermined, and peak locations are corrected for drift. When data acquistion begins, a unidirectional scan algorithm (*11*) is used to measure repetitively the major and minor isotopic ion beams either until the preset run time is exceeded or until the operator calls for termination of the run. If near-natural abundance measurements are being made, the gain of the I/F amplifier stage under computer control is switched from X1 for the major isotope to X100 for the minor isotope. During data acquisition, a real-time plot of either the major or minor isotope flux vs. time can be displayed on the lower half of the CRT screen, while a real-time plot of the isotope ratio can be displayed on the upper half.

After data acquisition terminates, a permanent copy of the data can be recorded on magnetic tape. To process the data, a first pass is made to define legitimate GC peaks and their boundaries. During this stage, the CRT can display a plot of the major or minor

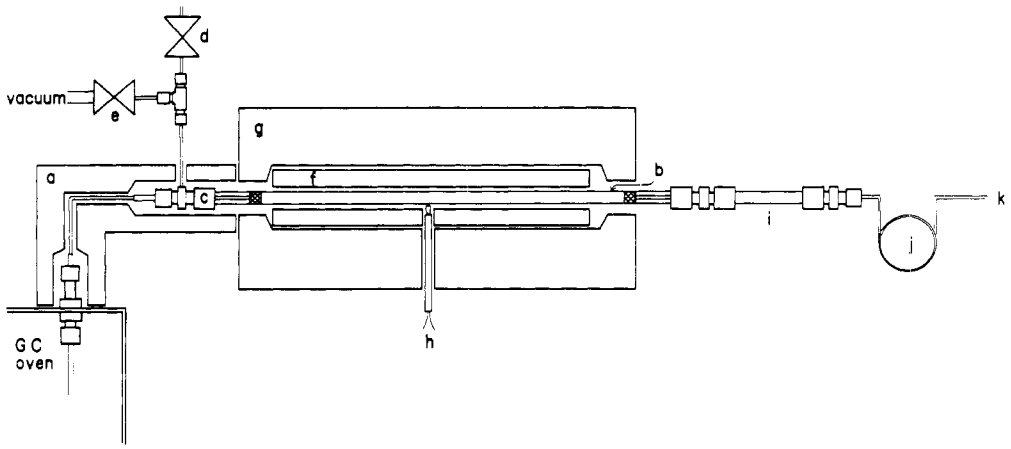

Figure 2. Diagram of combustion system. (a) Heating block (350 °C max) and transfer line (0.76 mm i.d. × 12 cm, stainless steel). (b) Combustion oven tube; 6 mm o.d. × 4 mm i.d. × 30 cm, Vycor. The central 22 cm is packed with 60–100 mesh cupric oxide (ground wire-form cupric oxide, Matheson, Coleman and Bell, Norwood, Ohio). A 3.5-cm length of 4-mm o.d. Pyrex tube (to reduce dead volume) and a 0.5-cm plug of quartz wool (to retain the cupric oxide) are placed in each end of the oven tube. (c) Union connecter modified with 0.25-mm i.d. sidearm for oxygen introduction or effluent diversion. (d) Valve to oxygen source. (e) Computer-controlled valve (12-VDC subminiature solenoid, Angar Scientific Corp., East Hanover, N.J.) for effluent diversion. (f) Furnace elements. (g) Insulation. (h) Chromel–alumel thermocouple. (i) Tube (6 mm o.d. × 7 cm, Pyrex) filled with magnesium perchlorate (G. F. Smith Chemical Co., Columbus, Ohio, used as obtained) retained by glass wool plugs. (j) Carbon dioxide trap, 1 mm i.d. × 1.6 mm o.d. × 40 cm, stainless steel; 1.5 turns of 3.5-cm diameter coil. (k) Connection to GCMS separator, 0.25 mm i.d. × 1 m, stainless steel

isotope flux vs. time on the lower half of the screen and a plot of the isotope ratio vs. time on the upper half of the screen. Furthermore, vertical lines will be drawn in the display to mark points at which chromatographic peak boundaries have been defined. Chromatographic peak boundaries are defined wherever the calculated slope (signal vs. time) for a moving window of data points rises above and falls below a preset trigger level. The slope of either the major isotope flux, the minor isotope flux, or the isotope ratio can be used for boundary definition.

The calculation of isotope ratios corresponding to the individual chromatographic peaks requires that background ion currents be taken into account. The software provides for determination of background ion currents using data just prior to the chromatographic peak, immediately following the peak, or by using an average of data from both these regions. The "background-corrected ion current ratio" is obtained by subtracting the background collecter currents from the observed total collecter currents for each ion beam, adjusting for amplifier gain differences, and forming a ratio of the integrated corrected currents. No corrections for mass discriminations occurring at any point in the instrumental system are made within the software (these problems are discussed in succeeding sections of this report).

Samples. From E. A. Vogler, Indiana University, two samples were received: one containing methyl octanoate, the other containing a mixture of methyl heptanoate, methyl octanoate, methyl nonanoate, methyl undecanoate, and methyl tridecanoate. Both samples were prepared by reacting the corresponding alkyl Grignard reagents with ^{13}C-enriched carbon dioxide. The acids were then esterified and diluted with *n*-pentane. The resulting esters are labeled with carbon-13 (≥85 at. %) in the carboxyl-carbon position. For methyl octanoate, intermediate levels of label incorporation were obtained by mixing the synthetic product with natural abundance material (≥99% pure, Analabs, Inc., North Haven, Conn.). Methyl nonanoate and methyl dodecanoate (≥99% pure, Applied Science Laboratories, State College, Pa.) were added as internal standards in the methyl octanoate and mixed-esters samples, respectively.

Amino acids derived from a nitrogen-15-enriched human serum albumin sample (*12*) were received from Dr. T. P. Stein, Graduate Hospital, University of Pennsylvania, Philadelphia, Pa. The amino acids had been converted to the *N*-acetyl, *n*-propyl ester derivatives (*13*, *14*).

Chromatography. The GC column used to separate methyl esters was a 2-mm i.d., 2-m long, stainless steel column packed with 6% FFAP on 120–150 mesh Gas Chrom Q. To resolve the C_7–C_{13} methyl esters, the column temperature was held at 100 °C for 2 min before programming at a rate of 8 °C/min to 190 °C. The injector and the transfer line between the GC and combustion line were held at 250 °C. A helium carrier gas flow rate of 19 mL/min was used. Samples containing only methyl octanoate in a pentane solvent were chromatographed isothermally at 100 °C.

The gas chromatographic separation of the amino acid derivatives was effected using a 2-mm i.d., 2-m long, stainless steel GC column packed with a mixed phase (0.3% Carbowax 20M, 0.3% Silar 5CP, and 0.05% Lexan) on Chromosorb W AW 120–140 mesh (*14*). The GC packing was obtained from J. Graff Associates (Santa Clara, Calif.). With the injector and the transfer line held at 250 °C and the helium carrier gas flowing at 20 mL/min, the best separation was achieved by holding the column temperature at 120 °C for 2 min before programming at a rate of 4 °C/min. When the phenylalanine derivative had eluted (~190 °C) the rate was increased to 32 °C/min to a maximum temperature of 250 °C.

Differential Isotope Ratio Analyses and Calculations. Conventional (*1*) dual inlet, dual collector measurements of carbon and oxygen isotopic abundances were made using a modified Varian GD-150 mass spectrometer (Varian MAT, GmbH, Bremen, West Germany) equipped with Nuclide EAH-300 electrometers and an IR-2a integrating digital voltmeter system (Nuclide Corporation, State College, Pa.). Results were corrected for ^{17}O-contributions at mass 45 and were expressed in terms of the PDB isotopic standard (PDB designates "Pee Dee Belemnite", a fossil carbonate used as a comparison point in isotopic abundance measurements, see ref. *15*).

RESULTS AND DISCUSSION

Combustion System Characterization. Many different combustion catalysts have been tested for use in quantitative elemental analysis, and many references on the subject can be found in the biennial reviews by Ma and Gutterson (*16*). A catalyst ideal for use with IRM-GCMS must: (a) produce quantitative combustion, (b) have a low operating temperature (no higher than 850 °C), and (c) not require a supplementary flow of oxygen. The first of these restrictions is imposed because nonquantitative combustion could be accompanied by isotopic fractionation and, more directly, because fragment ions arising from residual materials might appear at masses 28, 29, 44, or 45, thus causing serious errors in isotope ratio measurements. The second restriction is purely practical and is imposed because higher temperatures are difficult to maintain with a continuous 20 mL/min flow of helium carrier gas through the combustion furnace. The third restriction is imposed in order to minimize the problems associated with

Table I. Dependence of Combustion Efficiency on Reactor Temperature and Form of Oxidant

	combustion efficiency at indicated reactor temperature[a]			
oxidant	600 °C	700 °C	750 °C	800 °C
wire-form CuO	47%	83%	93%	99.7%
60–100 mesh CuO	87	99	>99.99	>99.99

[a] Tests carried out using 0.8 μmol CH_4, helium carrier gas flowing at 15 mL/min.

a continual flow of oxygen into the mass spectrometer. If the "catalyst" does not possess its own reservoir of available oxygen, then the supplementary oxygen flow must be large enough to ensure complete combustion of even large chromatographic peaks. The necessary flows would be substantial and could threaten the long-term stability of the mass spectrometer. The use of metal–oxide "catalysts", which continually degrade in order to support an equilibrium partial pressure of oxygen (and which thus function as reactants as well as catalysts in the combustion reaction), offers the best solution to this problem, providing oxygen on demand, but otherwise restricting oxygen flows to acceptable levels.

Since it has been demonstrated that it is particularly difficult to obtain quantitative combustion of methane (*17*), this compound acts as a convenient test substance which has been employed by previous workers (*17–19*) in studies of a variety of catalysts. A review of this previous work allowed the number of prospective catalysts to be reduced to three: cupric oxide, cobalt oxide (Co_3O_4), and the decomposition product of silver permanganate (*20*). Of the three, cupric oxide is the most readily available and easiest to prepare, and was chosen as the first to be tested for use with IRM-GCMS.

To measure the efficiency of the cupric oxide-filled combustion oven, methane was injected into the GC and masses 15 and 44 were monitored on alternate injections (mass 15, which carries about 40% of the total ion current in the spectrum of CH_4, was used to monitor methane because oxygen from the hot cupric oxide interfered at mass 16). Knowing the ratio of combusted methane (carbon dioxide, mass 44) to noncombusted methane (mass 15) and considering the fraction of the total CO_2 ion current at mass 44 and the fraction of the total CH_4 ion current at mass 15, the combustion efficiency of the oven could be calculated. Under the conditions prevailing in these experiments, the failure to detect any methane indicated a combustion efficiency of greater than 99.99%. The combustion efficiency was measured both for an oven filled with 60–100 mesh cupric oxide and for an oven filled with larger particle size (wire form) cupric oxide. Table I summarizes the test results as a function of oven temperature. As expected, increasing the catalyst temperature or increasing the catalyst surface area dramatically improved combustion efficiency. Because the heated cupric oxide particles tend to agglutinate with time, particles smaller than 100 mesh or particles of a narrow mesh range are not of great value. A 60–100 mesh cupric oxide-packed oven operated at 750 °C with a helium flow rate of 5–25 mL/min is suitable for IRM-GCMS use. Because of the success experienced with cupric oxide, alternate catalysts were not tested.

Although it obviously carries the information relating to the isotopic composition of the hydrogen in any sample materials, the water formed as a product of combustion can be troublesome in other respects, being particularly unwelcome as a needless input to the high vacuum system of the mass spectrometer. Water can be removed from the combustion effluent by placing a small trap (see Figure 2) of magnesium perchlorate at room temperature just after the cupric oxide furnace. Magnesium perchlorate not only has a large capacity for water, but the water is quantitatively removed from the effluent—for example, 1.2 μL of water injected directly into the combustion system causes no change in the mass 18 (water) background.

Carbon dioxide, which produces abundant fragment ions at masses 28 and 29, must be completely removed from the stream of combustion products when nitrogen isotopic abundances are to be measured. Ascarite ("soda-asbestos") has been used as a CO_2 absorbent in elemental analysis (*14*), but experience showed that this material could not be practically employed in this work in the same way that magnesium perchlorate functioned as a water absorbent. Instead, a short piece of stainless steel tubing dipped in liquid nitrogen was used to trap carbon dioxide while passing nitrogen unretained. When 2 μL of carbon dioxide was injected with the trap at liquid nitrogen temperature, no rise in the mass 44 baseline was recorded. When 50 μL of nitrogen was injected, the retention time of the peak was 36 s and the baseline width was 12 s, regardless of whether the trap had been cooled with liquid nitrogen or was at room temperature.

Several oxides of carbon and nitrogen are possible combustion products. To test for the production of carbon monoxide, 0.8 μmol of methane was injected into the GC and mass 28 monitored for the appearance of carbon monoxide. Carbon dioxide, which also produces mass 28 ions, was removed using the liquid nitrogen trap (methane is not retained). No evidence of carbon monoxide was found. To determine which nitrogen oxides form in the combustion tube, 0.57 μmol of 1-nitropropane was injected into the GC and the mass spectrum recorded during the elution of the GC peak. The only detectable nitrogen species were nitrogen and nitric oxide—no nitrogen dioxide, nitrous oxide, or other oxides.

Nitric oxide can be reduced to nitrogen by passage over hot copper metal (*21*), and it was therefore considered that it might be useful to place a copper-filled reactor in the gas stream following the combustion oven. To explore this possibility, the system was modified to include an Ascarite-filled trap and a copper-filled oven, both located between the water trap and the jet separator (see Figure 1). The use of fresh Ascarite provided efficient removal of CO_2 for brief periods of time, and made it possible to monitor mass 28 (N_2) and mass 30 (NO) without interference. This technique was necessary because the liquid-nitrogen trap normally used for CO_2 removal was found to retard nitric oxide very strongly. The copper-filled reduction reactor and furnace were identical to the cupric oxide-filled reactor tube and furnace. When 1.2 μmol of pyridine was injected into the GC, it was found that 98.2% of the nitrogen appeared as N_2 when the copper-filled reduction reactor was at 600 °C, 97.8% at 530 °C, 97.0% at 420 °C, and 93.6% at 120 °C. In the absence of any reduction system, a variety of other tests showed that at least 88% of the input nitrogen appeared as N_2. While these nonquantitative yields of N_2 would seriously distort quantitative elemental analyses, it has been tentatively concluded that they are acceptable in this application, and the system used in this work contained no NO_x-reduction reactor. The nonquantitative yield of N_2 does not significantly affect the sensitivity, and any isotopic fractionation involved should be quite constant and, therefore, of little consequence in any relative measurements. Furthermore, omission of the copper-filled reduction reactor removes a significant item of maintenance and minimizes dead volume and surface area in the system, thereby reducing peak broadening and minimizing memory effects between samples.

The equilibrium partial pressure of O_2 over CuO at 750 °C is 0.27 Torr (For a review of oxygen pressures in the system Cu, Cu_2O, CuO, O_2, see ref. 22), corresponding to the loss of only 4.5 mg oxygen per eight-hour period (assuming that the carrier-gas flow rate is 25 mL/min and that equilibrium is

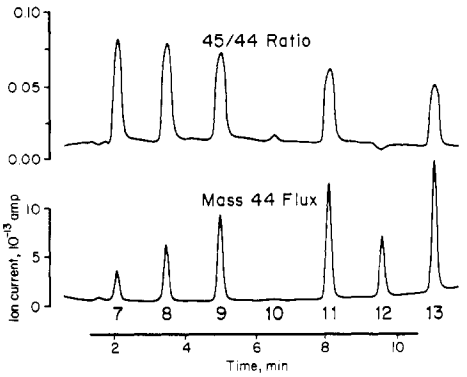

Figure 3. IRM-chromatograms for carbon isotope ratio measurements. Eluting are the methyl esters of normal alkanoic acids. The carbon numbers of the parent acids are given below the lower trace, which plots mass 44 ion current ($^{12}CO_2^+$) and which is representative, therefore, of the relative amounts of carbon (strictly, of ^{12}C) in each chromatographic peak. The upper trace plots the mass 45/mass 44 ion current ratio as a function of time. Positive deflections indicate increases in the abundance of mass 45 relative to mass 44 and, thus, the appearance of ^{13}C-labeled materials. Because it depicts only the variations in a *ratio*, the upper trace is not sensitive to the absolute amount of material entering the ion source or, therefore, to the relative concentrations of various materials in the injected mixture

maintained). Further considerations show that the primary demand on the oxygen reservoir is the combustion of organic sample materials, particularly the solvent peak, if it is allowed to reach the combustion oven. As noted (see Figures 1 and 2), this large load can be removed by diverting the solvent peak prior to the combustion oven. Consequently, the effective capacity of the combustion system is extremely high, and no evidence that the capacity has been approached has been observed in the present work, in which 1–2 mL/min of oxygen have been added to the helium carrier gas each night in order to regenerate the catalyst.

Carbon Isotopic Analyses. The obtainable levels of precision and the corresponding sample requirements were determined using a mixture of the methyl esters of the C_7, C_8, C_9, C_{11}, and C_{13} normal alkanoic acids. The carboxyl carbon atom in each acid was labeled with ^{13}C at a level of 85% or better, providing a series of peaks with between 6 and 10 at. % excess ^{13}C. In a separate series of experiments, methyl octanoate having natural isotopic abundance was mixed with small amounts of the labeled material in order to produce samples with less than 0.025 at. % excess ^{13}C, these samples being used to test performance at very low levels of enrichment.

The IRM-chromatogram of the mixed methyl esters sample is shown in Figure 3. The recording of the mass 44 ion current serves as a conventional chromatogram, and reveals distinct peaks for the methyl esters of the C_7, C_8, C_9, C_{11}, C_{12} (added as an unlabeled standard), and C_{13} *n*-alkanoic acids, as noted. The integrated mass 44 ion current for each peak is an accurate indicator of relative amounts of material for peaks differing only slightly in carbon isotopic abundance. However, when widely varying degrees of isotopic enrichment are encountered, it must be borne in mind that the total carbon flux is, in fact, strictly proportional to the *sum* of the ion currents at masses 44 and 45.

Full consideration of the 45/44 ratio recording is somewhat more complicated. While it is clear that the ion-current ratio observed at any time is simply the weighted average of the ion-current ratios for all the contributing species, the practical consequence of this fact is far-reaching: only qualitative information can be obtained from inspection of the plot itself, and extensive data processing is required for the extraction of accurate isotope ratios. These problems arise simply because contributions of the mass-spectrometer background

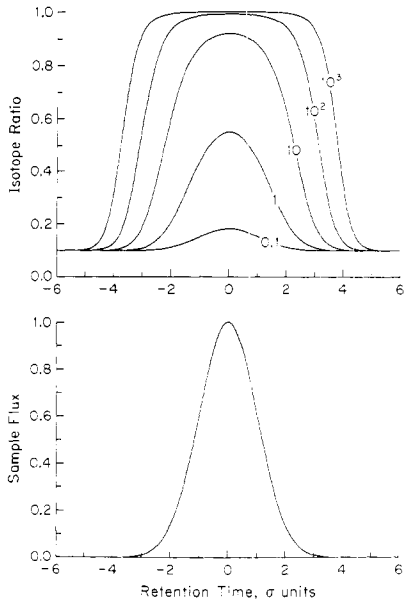

Figure 4. Idealized chromatographic peak and corresponding ion-current ratio plots. Each σ unit corresponds to one standard deviation in a Gaussian distribution, which is the assumed shape of the GC peak. The curves in the upper portion of the figure have been generated using Equation 1 at the various sample to background ratios indicated. The values of R_{bkgd} and R^* were arbitrarily set at 0.1 and 1.0, respectively.

to the ion currents as masses 44 and 45 cannot be ignored if high accuracy and sensitivity are to be obtained. A detailed discussion of this problem follows.

Mathematically summarizing the relationship between the observed ratio and sample and background ion currents, we can write

$$R(t) = \frac{[g(t)]R^* + bR_{bkgd}}{g(t) + b} \quad (1)$$

where $R(t)$ is the observed ion current ratio as a function of time, $g(t)$ is a function describing the shape of the gas chromatographic peak, b is a weighting factor [on the same scale as $g(t)$] proportional to the intensity of the background ion currents, R^* is the ion-current ratio pertaining to the sample itself, and R_{bkgd} is the ratio of the background ion currents. Figure 4 summarizes the results of calculations in which $g(t)$ was assumed to be Gaussian, R_{bkgd} was arbitrarily set at 0.1, R^* at 1.0, and the ratio of the maximum value of $g(t)$ to b was varied in the range $0.1 \leq [g(t)]_{max}/b \leq 10^3$ [that is, the (peak height/background) ratio was varied between 0.1 and 10^3]. It can be seen that $R(t)$ approaches R^* only for $g(t) \gg b$, and that $R(t)$ can be expected to vary significantly across the width of a chromatographic peak, even when R^* is constant across the peak.

If chromatographic resolution of isotropic species occurs, then R^* will not be constant across the width of the peak. Model calculations show that when isotopic species are separated by as little as 0.05 σ unit (*e.g.*, consider two Gaussian profiles like that in the lower half of Figure 4, their centers separated by 0.05 unit on the scale shown), pronounced asymmetry should be evident in the ratio plot even for sample/background ratios as low as 10. At higher sample/background ratios (e.g., the profile labeled "10^3" in Figure 4) the $R(t)$ vs. t plot should develop a distinct slope in the plateau region near its center.

The ion-current ratio plot in Figure 3 records distinct peaks (obvious ^{13}C enrichment) for the C_7, C_8, C_9, C_{11}, and C_{13} esters; a small peak apparently representing the C_{10} ester, which is nearly imperceptible in the mass 44 plot; and a small *negative* peak for the C_{12} ester standard.

Table II. Results of Replicate Analyses of Mixed Methyl Esters Sample

run	carbon number of parent acid						k_j
	C_7	C_8	C_9	C_{11}	C_{12}	C_{13}	
	background-corrected ion-current ratios						
1	0.13731	0.12493	0.11321	0.09666	0.01145	0.08419	0.9803
2	0.13780	0.12528	0.11381	0.09732	0.01153	0.08466	0.9871
3	0.13718	0.12566	0.11383	0.09814	0.01145	0.08445	0.9803
4	0.13773	0.12603	0.11425	0.09803	0.01152	0.08541	0.9863
5	0.13935	0.12587	0.11409	0.09825	0.01143	0.08529	0.9786
av	0.13788	0.12556	0.11384	0.09767	0.01148	0.08480	
std dev	0.00087	0.00045	0.00040	0.00070	0.00005	0.00053	
rel std dev, %	0.63	0.36	0.35	0.72	0.44	0.63	
	at. % ^{13}C						
av	12.248	11.272	10.323	8.981	≡1.081	7.882	
std dev	0.090	0.052	0.041	0.069		0.048	
rel std dev, %	0.73	0.46	0.40	0.77		0.61	
	at. % excess ^{13}C vs. C_9 internal standard						
av	1.925	0.949	≡0	−1.342	−9.242	−2.442	
std dev	0.062	0.013		0.031	0.041	0.023	
	sample amounts, nmol						
ester injected	0.54	0.97	1.31	1.43	≡0.62	1.41	
CO_2 produced	4.3	8.7	13.1	17.1	8.0	19.7	
	theoretical minimum relative std dev of measured ratio, %[a]						
	0.055	0.040	0.033	0.031	0.11	0.030	

[a] Assumes GC/MS interface efficiency is 10%. Based on Equation 7 (assumes shot-noise limiting). See text.

The C_{10} ester peak, which is apparent only in the ratio plot, and which was not expected on the basis of the planned synthesis, was traced to the presence of a 1-bromononane impurity in the alkyl halide mixture employed in the Grignard synthesis (see Experimental section). Although the impurity had escaped notice in a number of routine reaction-monitoring analyses, the ^{13}C-carboxylated product is hard to miss in the IRM-GCMS ratio plot. Quantitatively, the sensitivity of IRM-GCMS as a technique for detecting ^{13}C-labeled compounds can be judged by noting that the C_9 peak corresponds to 1.3 nmol of *ester* while the C_{10} peak represents only 16 pmol of ester. In this case, because $R^* \gg R_{bkgd}$, a minor impurity has become visible even though $g(t) < b$.

What causes the *negative* peak at C_{12} in the 45/44 ratio trace? Most simply, of course, it indicates that the 45/44 ion current ratio actually decreased when the C_{12}-ester-derived CO_2 entered the mass spectrometer. This decrease indicates that $R_{bkgd} > R^*$, a fact easily explained by noting that the background is due to a variety of species, and that in any practical circumstance the combined effect of these species will lead to a 45/44 ion-current ratio substantially greater than that in CO_2 having natural isotopic abundances. Even though the mass 44 recording shows the C_{12} ester to be far more abundant than the C_{10} contaminant, the deflections observed in the ratio plot are about equal. In the case of the C_{12} ester, the absence of any excess ^{13}C leads to a relatively small difference between R^* and R_{bkgd}, and this leads to a small deflection even though $g(t) \gg b$.

Quantitative results can be obtained by straightforward calculations based on the integrated mass 45 and mass 44 ion currents within each defined set of peak boundaries. For any chromatographic analysis, the relative concentrations of the various components can be determined from the *sums* of the integrated and background-corrected mass 44 and mass 45 signals, while the isotope ratios can be calculated from the *ratios* of the integrated and background-corrected mass 44 and mass 45 signals. For the particular case illustrated by Figure 3, a known amount of methyl dodecanoate has been added as an internal standard. In such circumstances, assuming that the number of carbon atoms per molecule is known for each peak, it is possible to calculate absolute amounts for all species present, separate calibrations not being required because CO_2 is the species used to quantify all compounds. Using the symbol ^{45}R to denote the background-corrected 45/44 ion current ratio, and the symbols ^{13}R and ^{17}R to denote ($^{13}C/^{12}C$) and ($^{17}O/^{16}O$) respectively, we can write

$$^{45}R_{ij} = k_j(^{13}R_i + 2\,^{17}R) \quad (2)$$

where k is a constant taking into account the various mass discrimination effects (faster pumping of $^{12}CO_2$ from the ion source, different ion extraction and transmission efficiencies for m/e 44 and m/e 45, different electron multiplier gains for m/e 44 and m/e 45). The subscripts i and j are used to denote components and chromatographic runs, respectively, with $^{45}R_{ij}$ denoting the observed, background-corrected 45/44 ion-current ratio for the ith component in the jth run. Because k can depend on ion source focusing conditions, it cannot be regarded as perfectly constant, and must be evaluated separately for each run. No subscript is assigned to ^{17}R because the oxygen isotopic composition established by the combustion oven is assumed to be equal for all samples.

Background-corrected ion current ratios for five replicate runs of the mixed methyl esters sample are shown in Table II. The relative standard deviations of these raw ratios range from 0.4 to 0.7%. Expressed in terms of at. % ^{13}C [$\sim 100R/(1 + R)$], these same standard deviations correspond to 0.005 to 0.06 at. % ^{13}C. The calculation of carbon isotopic abundances, however, requires knowledge of $^{13}R_i$ values, and these must be calculated using some approach based upon Equation 2. Given $^{45}R_{ij}$, calculation of $^{13}R_i$ requires knowledge of k_j and ^{17}R.

The value of ^{17}R can be calculated from the oxygen-isotopic abundances observed in the products of similar combustion systems. Typically, we find $\delta^{18}O_{SMOW}$ values in the range +10 to +30‰,

$$\delta^{18}O_{SMOW} = [(^{18}R_x - {}^{18}R_{SMOW})/{}^{18}R_{SMOW}]\ 10^3 \quad (3)$$

in this expression, ^{18}R designates the ratio ($^{18}O/^{16}O$), the subscript x designates an unknown sample, and SMOW designates "standard mean ocean water", the isotopic reference material for oxygen. The relationship between ^{17}O and ^{18}O abundances is given by (*15*).

$$(^{18}R_a/^{18}R_b)^{1/2} = (^{17}R_a/^{17}R_b) \quad (4)$$

where the subscripts a and b designate any two oxygen pools. Equations 3 and 4 allow calculation of ^{17}R in the following way: (i) ^{18}R values in the combustion products (equivalent to $^{18}R_x$ in Equation 3) can be determined using the observed range of $\delta^{18}O_{SMOW}$ values and $^{18}R_{SMOW} = 1.9968 \times 10^{-3}$ (*23*); (ii) $^{17}R_{SMOW}$, although not known directly, can be found using Equation 4, $^{18}R_{SMOW}$, and the values $^{18}R_{PDB} = 2.0790 \times 10^{-3}$ (*15*), and $^{17}R_{PDB} = 3.7995 \times 10^{-4}$ (*15*); (iii) ^{17}R values for the combustion products can be found using Equation 4, $^{17}R_{SMOW}$, $^{18}R_{SMOW}$, and the results of step (i). We find $3.74 \times 10^{-4} \leq {}^{17}R \leq 3.78 \times 10^{-4}$. Because the combustion products average $\delta^{18}O_{SMOW} = +15‰$, we adopt $^{17}R = 3.75 \times 10^{-4}$.

The value of k_j can be calculated by applying Equation 2 in a case in which k_j is the only unknown. In the present work, it is known from differential isotope ratio analyses that $\delta^{13}C_{PDB}$ for the methyl dodecanoate is −27.3‰ where

$$\delta^{13}C_{PDB} = [(^{13}R_x - {}^{13}R_{PDB})/{}^{13}R_{PDB}]\ 10^3 \quad (5)$$

Given $^{13}R_{PDB} = 0.0112372$ (*15*), we calculate $^{13}R = 0.010930$ for the methyl dodecanoate, allowing the calculation of the various k_j values reported in Table II.

Using Equation 2 and the known values of ^{17}R and k_j, it is then possible to calculate $^{13}R_i$ values, and, in turn, atomic percentages based on the relationship (at. % ^{13}C) = $100^{13}R/(1 + {}^{13}R)$. The results of these calculations are given under the heading, "at. % ^{13}C" in Table II. Within each run, it is possible to compute the at. % excess ^{13}C for each acid in comparison to the C_9 acid, thus using the latter as an internal standard or reference point. As shown in the table, this procedure appreciably reduces the scatter between runs. For example, the standard deviation of the absolute ^{13}C abundance for the C_{11} acid is 0.069 at. % ^{13}C, while the standard deviation of the differential quantity (at. % excess ^{13}C vs. C_9) corresponds to 0.031 at. % ^{13}C. Because most real situations deal with exactly this kind of differential comparison (as opposed to an absolute measurement), it is this measure of precision which has greater practical significance.

The precision of any ion-current ratio measurement depends very substantially on the number of ions collected during the course of the observation (*24*). If we consider, as a useful reference point, the precision expected in a ratio measurement limited only by ion-beam shot noise, it can be shown that the relative variance in the ratio $R = F_2/F_1$, in which F_1 and F_2 represent the fluxes of the major and minor ion beams, respectively, is given by

$$v_R^2 = (\sigma_R/R)^2 = N_1^{-1} + N_2^{-1} \quad (6)$$

where v_R designates the coefficient of variation or relative standard deviation and N_1 and N_2 represent the numbers of ions collected from the major and minor ion beams, respectively. If it is assumed that the ratio is measured by switching the ion beam between masses at a single collector, and that the observation times are divided optimally (*24*), such that $t_1/t_2 = \sqrt{R}$, then it can be shown that

$$v_R^2 = (1 + 2R^{1/2} + 2R + 2R^{3/2} + R^2)/MRE \quad (7)$$

where M represents the total number of sample molecules introduced to the mass spectrometer during the measurement and E represents the overall mass spectroscopic efficiency (ions collected/molecule introduced).

The relative standard deviations of ratio measurements actually found in this work can be compared to theoretical maximum performance levels calculated using Equation 7. In order to carry out this calculation, we note that the value of R is measured directly, that M can be determined from the sample amounts calculated by reference to the C_{12} internal standard (we will assume that the GCMS interface actually transmits 10% of the combustion-produced CO_2 to the ion source), and that E is known to have a value of approximately 2×10^{-7} ion/molecule for carbon dioxide under the conditions employed in these measurements. The resulting theoretical minimum relative standard deviations are given as the last row of entries in Table II. It can be observed that the actual performance falls short of that theoretically attainable by a factor of from 4 to 20. This relatively low performance cannot be accounted for simply in terms of electronic noise sources (*24*) not considered in the derivation of Equation 7, and must represent the effect of some other uncontrolled variations in the measurement procedure. In particular, the fact that enriched samples fall short of the theoretically attainable precision by a greater margin than near-natural abundance samples suggests that the measurement of and correction for the background are of particular importance. The magnitude of errors associated with this process would be expected to increase as the ratios of the sample and background differed more and more strongly, and as the background became more intense, and exactly this behavior is observed.

It is apparent that IRM-GCMS is capable of reasonably high precision, and it is indicated both by practical experience (Table II) and theory (Equation 7) that the attainable precision should improve as ^{13}R tends toward natural abundance levels. In these circumstances, it is interesting to ask how successfully the technique can be applied to measurements of natural isotopic abundance variations. To prepare a sample with a very small ^{13}C enrichment, a large excess of unenriched methyl octanoate was added to the methyl octanoate sample which was >85% ^{13}C-labeled in the carboxyl carbon. The new sample, designated sample A, was expected to have a 0.17 at. % excess ^{13}C in the carboxyl carbon position, but less than 0.025 at. % excess ^{13}C overall. The carbon isotope ratios for sample A and for a sample of unenriched (natural isotopic abundance) methyl octanoate were determined by IRM-GCMS. Triplicate observations, each using 9 nmol of methyl octanoate, gave $^{13}R = 0.010581$ ($s_{mean} = 0.000010$) for the unenriched sample and $^{13}R = 0.011066$ ($s_{mean} = 0.000003$) for sample A, corresponding in this case to 0.0215 ($s = 0.0011$) at. % excess ^{13}C in the enriched sample. In the context of measurements near natural isotopic abundance, the performance of IRM-GCMS is best judged by asking how accurately this small difference has been evaluated.

A comparison of the same two samples using conventional dual inlet, dual collecter isotope ratio mass spectrometry provides an independent evaluation of the isotope ratio difference. For this analysis, carbon dioxide was produced off-line using a post-column GC-combustion system like that used in IRM-GCMS, with the carbon dioxide being trapped in break-seal tubes for transfer to the mass spectrometer inlet system. Triplicate observations, each using 0.23 μmol of methyl octanoate, gave $\delta^{13}C_{PDB} = -30.0‰$ ($s_{mean} = 0.15‰$) for the unenriched sample and $\delta^{13}C_{PDB} = -9.6‰$ ($s_{mean} = 0.10‰$) for sample A. Translating (Equation 5) these results in terms of atom % ^{13}C, the difference between the samples corresponds to 0.0224 ($s = 0.0002$) at. % excess ^{13}C in the enriched sample. The accuracy of the IRM-GCMS measurement is supported by the failure to find any significant difference between it and the conventional measurement, and it appears that differences as small as 0.002 at. % ^{13}C can be resolved

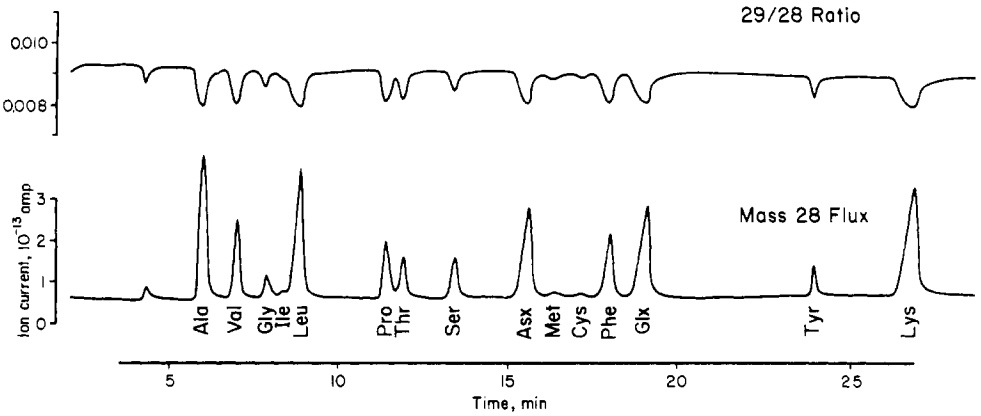

Figure 5. IRM-chromatograms for nitrogen isotope ratio measurements. Eluting are the *N*-trifluoroacetyl, *n*-propyl ester derivatives of amino acids derived from the hydrolysis of ^{15}N-enriched human serum albumin

Table III. Measurement of Excess ^{15}N in Amino Acids from Human Serum Albumin

amino acid	mass 28 normalized peak area	residues per albumin molecule[b]	contribution to total analyzed nitrogen, %[c]	mass 29/-mass 28 ratio × 100	std dev of ratio × 100[d]	^{15}N at. % excess ± 95% confidence limits[e]
Ala	16.0	63	11.2	0.7943	0.003	0.029 ± 0.001
Val	4.7	39	7.0	0.7863	0.009	0.025 ± 0.006
Gly	2.1	12	2.1	1.0697	0.022	0.165 ± 0.014
Ile		8	1.4 } 12.3			
Leu	12.5	61	10.9 }	0.7665	0.004	0.015 ± 0.002
Pro	4.9	25	4.5	0.7708	0.005	0.018 ± 0.004
Thr	1.5	30	5.4	0.7415	0.019	0.003 ± 0.012
Ser	2.1	22	3.9	1.0263	0.034	0.144 ± 0.021
Asp	9.4	54	9.6	0.7874	0.003	0.026 ± 0.003
Phe	3.6	30	5.3	0.7728	0.016	0.019 ± 0.010
Glu	19.9	83	14.8	0.7849	0.003	0.025 ± 0.003
Tyr	2.4	18	3.2	0.7748	0.013	0.020 ± 0.009
Lys	22.9	58	20.7	0.7357	0.003	≡0.0
	100.0	503	100.0			

[a] One normalized peak area unit corresponds to 10.5 nmol N_2. [b] Based on the composition reported in ref. 22. [c] Based on molar ratios in preceding column, excludes nitrogen present in albumin but not analyzed in this experiment, see text. [d] Reported standard deviation refers to the population of individual analyses. Based on five observations of each ratio. [e] Mean of five results. Confidence limits given by 2.78 (std dev individual at. % excess results)/$\sqrt{5}$.

near natural abundance. This difference corresponds to 0.2 pmol excess ^{13}C in a sample containing 10 nmol of carbon.

Nitrogen Isotopic Measurements. To test the ability of the IRM-GCMS system to determine nitrogen isotope ratios at low levels of ^{15}N enrichment, we obtained from Dr. T. P. Stein amino acids derived from a serum albumin sample in which the excess ^{15}N in any amino acid was expected to be less than 0.2 at. % (*12*). The IRM-GCMS chromatogram for the serum albumin amino acids is presented in Figure 5. The lower trace is a plot of mass 28 ion current vs. time; the upper trace is a plot of the mass 29/28 ion-current ratio vs. time. The mass 28 flux responds only to nitrogen-containing compounds, with peak area being proportional to the concentration of the species eluting and to the number of nitrogen atoms it contains. In parallel with the 45/44 ratio plot in the case of carbon, the 29/28 ratio plot records compounds containing near-natural-abundance nitrogen isotopes as negative peaks. This occurs because the background ion currents, which receive contributions from a variety of species in addition to N_2, give rise to a 29/28 ratio slightly greater than that characteristic of near-natural-abundance N_2. Peaks with significant levels of ^{15}N enrichment would register, of course, as positive peaks in the same fashion as shown for ^{13}C-enriched compounds in Figure 3, and, in general, the same considerations discussed in connection with calculations based on carbon isotopic data must be applied in the case of nitrogen analyses.

The identification of each GC peak in Figure 5 is based on retention time data and expected peak size for each amino acid. Quantitative data pertaining to the analysis are summarized in Table III. The first three columns list the background-corrected, integrated, normalized, mass 28 peak areas for each acid; the number of residues of each acid in the protein (*25*); and the contribution which each amino acid is expected to make to the total nitrogen analyzed. Comparison of the first and third columns indicates reasonable quantitative agreement, particularly for the relatively nonpolar amino acids. Not all of the nitrogen present in serum albumin is represented in Table III; species missing are: tryptophan (destroyed during protein hydrolysis); methionine (present in only small quantities in serum albumin); arginine, cysteine, and histidine (lost during sample preparation); and the amide nitrogen of glutamine and asparagine (also lost during sample preparation). Using specialized conditions, the nitrogen isotopic composition for any of these species could be measured.

The nitrogen isotope ratio, $^{15}R = (^{15}N/^{14}N)$, is related to the observed ion current ratio, $^{29}R = (29/28)$, by an expression similar to Equation 2.

$$^{29}R_{ij} = k'_j(2\,^{15}R_i) \qquad (8)$$

where a constant, k, is again introduced to account for a variety of mass discrimination effects, where the subscripts i and j again denote components and runs, respectively, and where the coefficient 2 appears because the molecular ion contains

two nitrogen atoms. Table III presents the average of five observations of ^{29}R for each amino acid and tabulates average ^{15}N excesses based on the following expression

$$\Delta P_{ij} = \left(\frac{^{15}R_{ij}}{1 + {}^{15}R_{ij}} - \frac{^{15}R_{\mathrm{lys},j}}{1 + {}^{15}R_{\mathrm{lys},j}} \right) 100 \qquad (9)$$

where ΔP_{ij} denotes the at. % excess ^{15}N observed in the ith amino acid in the jth chromatographic run. Lysine was used as the internal standard of assumed natural isotopic abundance because it has been shown not to become enriched in ^{15}N in metabolic experiments of this type (*26, 27*). The at. % excess results given in Table III represent the means of five replicate observations obtained by making five injections of the mixture and carrying out five analyses, applying Equation 9 to each individually. The reported confidence intervals are based on the observed standard deviations of the replicate atom percent excess results, and cannot be calculated directly from the standard deviations of the mass 29/mass 28 ratios. The reported confidence intervals are based on the observed standard deviations of the replicate atom percent excess results, and cannot be calculated directly from the standard deviations of the mass 29/mass 28 ratios.

The ^{15}N at. % excess values for the serum albumin amino acids range from 0–0.165%. As expected from the conditions of the experiment (*12*), the bulk of the ^{15}N is incorporated into glycine and serine, with only very minor incorporation into the other acids. To check the accuracy of these numbers, the ^{15}N at. % excess for glycine has been determined by an independent method, optical emission spectroscopy (*12*) to be 0.165 ± 0.05% (*28*). The IRM-GCMS ^{15}N at. % excess value of 0.165 ± 0.014% is in good agreement.

The results in Table III suggest that the precision of nitrogen isotopic analyses by this method falls short of that attainable with carbon samples of equal size. Nevertheless, only 100 nmol of N_2 are required to obtain a relative standard deviation of 0.5%. At natural abundance, a 0.5% change in the isotope ratio corresponds to 0.004 at. % excess ^{15}N, or 4 pmol excess ^{15}N in a sample containing 100 nmol of nitrogen.

The data presented in Table III are unique, IRM-GCMS presently being the only method which can determine low level ^{15}N enrichments in a mixture of amino acids in a single analysis. Alternative methods require that the individual amino acids be isolated, individually converted to N_2, and separately analyzed by mass or emission spectrometry, the time requirements quite probably exceeding 40 h. Using IRM-GCMS, the ^{15}N enrichments in a mixture of derivatized amino acids can be determined as the GC peaks elute. IRM-GCMS is applicable not only to amino acids, but to any *nitrogen-containing compound* that can be chromatographed.

ACKNOWLEDGMENT

The authors thank T. P. Stein, the Graduate Hospital, University of Pennsylvania, for preparing the amino acid samples from his human serum albumin studies. We appreciate the assistance of our co-workers E. A. Vogler, who prepared the labeled ester samples, and W. C. Qualls and T. W. Kammer, who carried out the conventional isotopic analyses of the natural abundance methyl octanoate.

LITERATURE CITED

(1) C. R. McKinney, J. M. McCrea, S. Epstein, H. A. Allen, and H. C. Urey, *Rev. Sci. Instrum.*, **21**, 724 (1950).
(2) C. C. Sweeley, W. H. Elliott, J. Fries, and R. Ryhage, *Anal. Chem.*, **38**, 1549 (1966).
(3) M. Sano, Y. Yotsui, H. Abe, and S. Sasaki, *Biomed. Mass Spectrom.*, **3**, 1 (1976).
(4) J. Franc and M. Wurst, *Collect. Czech. Chem. Commun.*, **25**, 701 (1960).
(5) F. Cacace, R. Cippollini, and G. Perez, *Science*, **132**, 1253 (1960).
(6) A. T. James and E. A. Piper, *J. Chromatogr.*, **5**, 265 (1961).
(7) J. Winkleman and A. Karmen, *Anal. Chem.*, **34**, 1067 (1962).
(8) F. Cacace, R. Cipollini, and G. Perez, *Anal. Chem.*, **35**, 1348 (1963).
(9) D. A. Schoeller and J. M. Hayes, *Anal. Chem.*, **47**, 408 (1975).
(10) T. A. Woodruff and H. V. Malmstadt, *Anal. Chem.*, **46**, 1162 (1974).
(11) D. E. Matthews and J. M. Hayes, *Anal. Chem.*, **48**, 1375 (1976).
(12) T. P. Stein, M. J. Leskiw, and H. W. Wallace, *Am. J. Physiol.* **230**, 1326 (1976).
(13) J. Graff, J. P. Wein, and M. Winitz, *Fed. Proc., Fed. Am. Soc. Expt. Biol.*, **22**, 244 (1963).
(14) R. F. Adams, *J. Chromatogr.*, **95**, 189 (1974).
(15) H. Craig, *Geochim. Cosmochim. Acta*, **12**, 133 (1957).
(16) T. S. Ma and M. Gutterson, *Anal. Chem.*, **48**, 101R (1976).
(17) S. Ebel, *Fresenius' Z. Anal. Chem.*, **264**, 16 (1973).
(18) J. Horacek, J. Korbl, and V. Pechanec, *Mikrochim. Acta*, **1960**, 294.
(19) V. Pechanec, *Collect. Czech. Chem. Commun.*, **32**, 2917 (1973).
(20) J. Korbl, *Mikrochim. Acta*, **1956**, 1706.
(21) G. Kainz and K. Zidek, *Microchim. Acta*, **1967**, 725.
(22) *Gmelins Handb. der Anorg. Chem., Kupfer*, **B1**, 31 (1958).
(23) P. Baertschi, *Earth Planet. Sci. Lett.*, **31**, 341 (1976).
(24) D. W. Peterson and J. M. Hayes, In "Contemporary Topics in Analytical and Clinical Chemistry", Vol. 3, D. M. Hercules et al., Ed., Plenum Press, New York, N.Y., in press.
(25) T. Peters, in "The Plasma Proteins", Vol. 1, F. W. Putnam, Ed., Academic Press, New York, N.Y., 1975, p 141.
(26) Y. Sheng, T. M. Badger, J. M. Asplund, and R. L. Wixom, *J. Nutr.*, **107**, 621 (1977).
(27) D. Halliday and R. O. McKeran, *Clin. Sci. Molec. Med.*, **49**, 581 (1975).
(28) T. P. Stein, Graduate Hospital, University of Pennsylvania, Philadelphia, Pa., personal communication.

RECEIVED for review March 2, 1978. Accepted June 9, 1978. We appreciate the support of the National Institutes of Health (GM-18979) and the National Aeronautics and Space Administration (NGR 15-003-118).